Journal of Information System and Technology Management
EISSN: 0128-1666
JISTM
Volume 6 Issue 24 (December 2021) PP. 152-160
DOI: 10.35631/JISTM.624016


JOURNAL OF INFORMATION SYSTEM AND TECHNOLOGY MANAGEMENT (JISTM)
www.jistm.com

# DETECTION OF EQUATORIAL PLASMA BUBBLES USING GPS IONOSPHERIC TOMOGRAPHY OVER PENINSULAR MALAYSIA

Siti Syukriah Khamdan[1*], Tajul Ariffin Musa[1], Suhaila M. Buhari[1,2]

[1] Geomatic Innovation Research Group (GnG), Faculty of Built Environment and Survey, Universiti Teknologi Malaysia, Malaysia
Email: syukriahkhamdan91@gmail.com; tajulariffin@utm.my
[2] Department of Physics, Faculty of Science, Universiti Teknologi Malaysia, Malaysia
Email: suhailamb@utm.my
[*] Corresponding Author

**Article Info:**

**Article history:**
Received date: 01.10.2021
Revised date: 01.11.2021
Accepted date: 20.11.2021
Published date: 01.12.2021

**To cite this document:**

Khamdan, S. S., Musa, T. A., & Buhari, S. M. (2021). Detection Of Equatorial Plasma Bubbles Using GPS Ionospheric Tomography Over Peninsular Malaysia. *Journal of Information System and Technology Management, 6* (24), 152-160.

**DOI:** 10.35631/JISTM.624016



**Abstract:**

This paper presents the detection of the equatorial plasma bubbles (EPB) using the Global Positioning System (GPS) ionospheric tomography method over Peninsular Malaysia. This paper aims to investigate the capability of the GPS ionospheric tomography method in detecting the variations of the EPB over the study area. In doing so, a previous case study during post-sunset 5th April 2011 has been selected as a reference for the detection of the EPBs over the study area. It has been observed that at least three structures of the EPBs have been captured based on the rate of change total electron content (TEC) index (ROTI) from 12 UT until 19 UT. Therefore, the three-dimensional ionospheric profiles have been reconstructed over Peninsular Malaysia using the tomography method during the study period in order to capture the signature of the EPBs. In this study, the detection of the EPBs using the tomography method is based on the rate of change of electron density (ROTNe). The results from three-dimensional ionospheric tomography show only two structures of EPBs are detected during the study period. It has been observed that the ROTNe depleted up to ~-12x109el/cm. Overall, the results in this study show that the GPS ionospheric tomography capable to be utilized in detecting the variations of EPBs in support of ionospheric studies and monitoring in the Malaysian region.

**Keywords:**

Global Positioning System, Tomography, Equatorial Plasma Bubbles, GPS Ionospheric Tomography

Journal of Information System and Technology Management
EISSN: 0128-1666
JISTM
Volume 6 Issue 24 (December 2021) PP. 152-160
DOI: 10.35631/JISTM.624016

## Introduction

The ionospheric conditions over the equatorial region are considered unique compared to the middle and high latitude region (Oryema *et al.*, 2016). This may due to the low inclination of the geomagnetic field lines and the increasing/decreasing of the electron density which controlled by the strength of electric current from the lower part of the ionospheric layer such as E-layer (Abdu, 2016). The equatorial ionosphere region is common with the occurrences of ionospheric special features or irregularities such as the equatorial electrojet (EEJ) (Amechi *et al.*, 2020), equatorial plasma bubbles (EPB) (Sarudin *et al.*, 2017; Tsunoda, 2015), equatorial spread-F (ESF) (Huba and Liu, 2020; Gurram *et al.*, 2018), equatorial ionization anomaly (EIA) (Khamdan *et al.*, 2019; Patel *et al.*, 2017), field aligned irregularities (FAI) Martiningrum *et al.*, 2020) and others.

The EPB, associated with the night-time irregularities, which initiated during the post-sunset and lasted up to few hours and sometime will be extended up to the topside of the ionosphere layer (Aa *et al.*, 2020; Mersha *et al.*, 2020). This irregularity is initiated through the generalized Rayleigh-Taylor instability (RTI) mechanism, where it is an instability of an interface between two layers with different densities which occurs when the lighter layer is pushing the heavier layer (Nade *et al.*,2020). Since the peak of the electron density are located around 350 km to 450 km above the Earth's surface, this layer is supported by the lighter layer of the electron density at the bottom-side of the ionosphere F-layer.

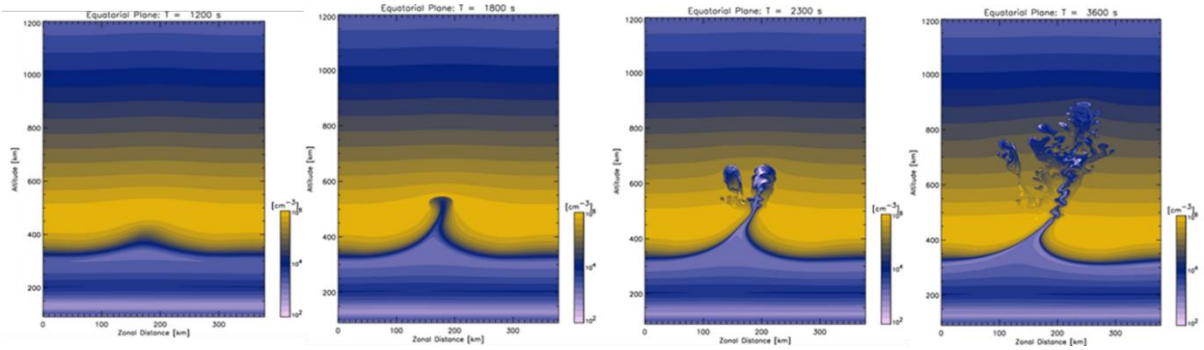


**Figure 1: Illustration of The Bubbles from Bottom to Upper Layer of Ionosphere**

(Source: National Institute of Information and Communication (NICT), 2021).

Figure 1 shows the illustration of the initiation of the bubbles from the bottom layer (lighter densities) to upper layer (heavier densities) of the ionosphere. In the evening, due to recombination of the bottom-side of the ionosphere, its density become unstable and triggered the RTI mechanism. Based on Kil (2015), the perturbation that initiated in the bottom ionosphere F-layer rise like a bubble and penetrates the top layer of the ionosphere. Then, the occurrences of irregularities not only can be observed along the trace of the bubbles, but also within and around the rising bubbles.

The EPB structure is determine based on depletion of the electron density with respect to the background ionosphere at the bottom F-layer. It produces a broad scale of ionospheric irregularities with a scale size from meters to hundreds of kilometres and highly affected by local time, longitude, seasonal, solar cycle and geomagnetic activity (Buhari *et al.*, 2014; Tsunoda *et al.*, 2014). The development and movement of EPB is controlled by the electric

Journal of Information System and Technology Management
EISSN: 0128-1666
Volume 6 Issue 24 (December 2021) PP. 152-160
DOI: 10.35631/JISTM.624016

field, reduction of ionosphere E-layer conductance at night and occurrence of the pre-reversal enhancement after sunset (Timocin *et al.*, 2020; Abadi *et al.*, 2015; Magdaleno *et al.*, 2015). Previously, the EPB structure are detected using an airglow imager, incoherent scatter radar and ionosonde. However, due to the limited spatial imaging coverage of those instruments (Fukao *et al.*, 2006; Yokoyama *et al.*, 2004), the Global Positioning System (GPS) has been used in order to detect the EPBs structure. With a dense network of GPS all over the globe, it is an advantage for GPS to monitor the structure of the EPBs as it grows to the topside of the F-layer and has a larger width at the bottom-side of the ionosphere (Buhari *et al.*, 2014). Following the current trend of research, the three-dimensional structure of the EPBs has been observed (Kil, 2015; Yokoyama *et al.*, 2015).

Therefore, by using a dense network of GPS, this study will observe the three-dimensional structure of EPBs using the GPS ionospheric tomography method over the study area. The tomography method from Khamdan *et al.* (2020) will be used to reconstruct during post-sunset 5th April 2011 to observe the three-dimensional EPBs structures based on the previous study as presented by Buhari *et al.* (2014) over the Peninsular Malaysia.

**Determination of EPB using GPS Tomography Method**

During 5th April 2011, Buhari *et al.* (2014) has been observed several structured of EPBs over the Southeast Asian region. The detection of the EPBs is based on the TEC-derived from GPS measurements where large depletion of the electron densities creates the EPBs form after sunset cause the TEC to fluctuate or depleted. In order to differentiate the small-scales depletion of the TEC due to the EPBs, the rate of change TEC index (ROTI) has been used at 5 minutes intervals (Sarudin *et al.*, 2017; Buhari *et al.*, 2015; Nishioka *et al.*, 2008). The ROTI is defined as the standard deviation of the TEC difference, the so-called rate of TEC change (ROT) which mathematically derived as below (Buhari et al., 2014;).

$$ROT = \left(\frac{TEC_{t+\Delta t} - TEC_t}{\Delta t}\right) \quad (1)$$

where $t$ is time and $\Delta t$ is 30 seconds intervals. Then, the ROTI map or known as keogram can be generated in order to detect the irregularities (Yokoyama *et al.*, 2004).

In this study, a dense GPS network over Peninsular Malaysia has been utilized to reconstruct the three-dimensional ionospheric profile over the study area. The tomography method that was used in this study are based on Khamdan et al. (2020). Since, the ionospheric tomography method providing the ionospheric profiles in term of electron density, therefore, to serve the purposes of this study, a modification of Equation 1 as proposed by Khamdan (2018) has been made in order to estimate the rate of change of electron density ($ROT_{Ne}$). Equation 2 shows the mathematical equation of $ROT_{Ne}$.

$$ROT_{Ne} = \left(\frac{N_{e_{t+\Delta t}} - N_{e_t}}{\Delta t}\right) \quad (2)$$

where $N_e$ represents the electron density. Figure 2 shows the workflow of the reconstruction of the GPS ionospheric tomography in detection of EPBs structures. To serve the purposed of the study, the reconstruction of three-dimensional ionospheric tomography will be reconstructed after the local post-sunset within 12 UT to 19 UT with 1 hour interval. Up to the author knowledge, there are no studies that have reported monitoring the EPBs structure in terms of three-dimensional and utilizing the tomography method over the study area. The ROTI

Journal of Information System and Technology Management
JISTM
EISSN: 0128-1666
Volume 6 Issue 24 (December 2021) PP. 152-160
DOI: 10.35631/JISTM.624016

maps from the previous study will be used as a reference in order to detect the occurrences of the EPBs structure over the study area. Meanwhile, for the tomography method, the detection of the EPBs structure will be based on depletion of electron density from $ROT_{Ne}$ maps.

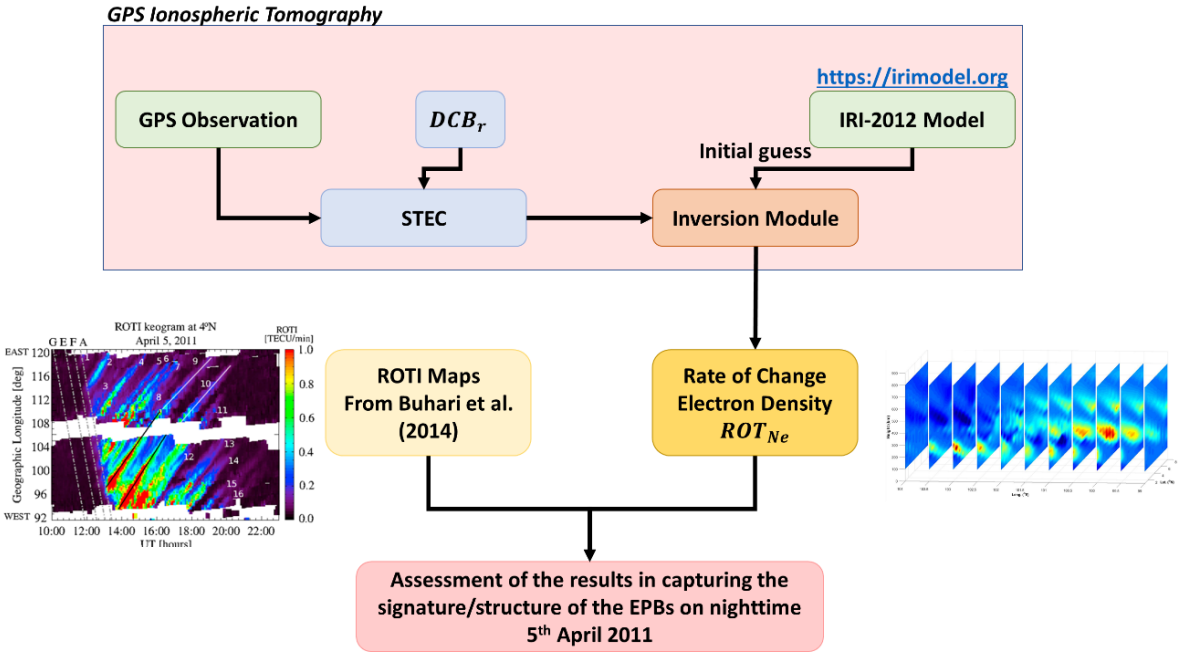


**Figure 2: Workflow of The Reconstruction of GPS Ionospheric Tomography to Detect The Structure of The EPBs.**

## Results and Analysis

Buhari *et al.* (2014) has been observed at least 16 striations of the EPBS on the night-time over the 4°N that covered the Southeast Asian region. It has been observed that during the study period, low solar activity with low values of Kp-index has been reported. Figure 3 shows the results from Buhari *et al.* (2014) that has been generated for every 5 minutes.

Journal of Information System and Technology Management
EISSN: 0128-1666
Volume 6 Issue 24 (December 2021) PP. 152-160
DOI: 10.35631/JISTM.624016

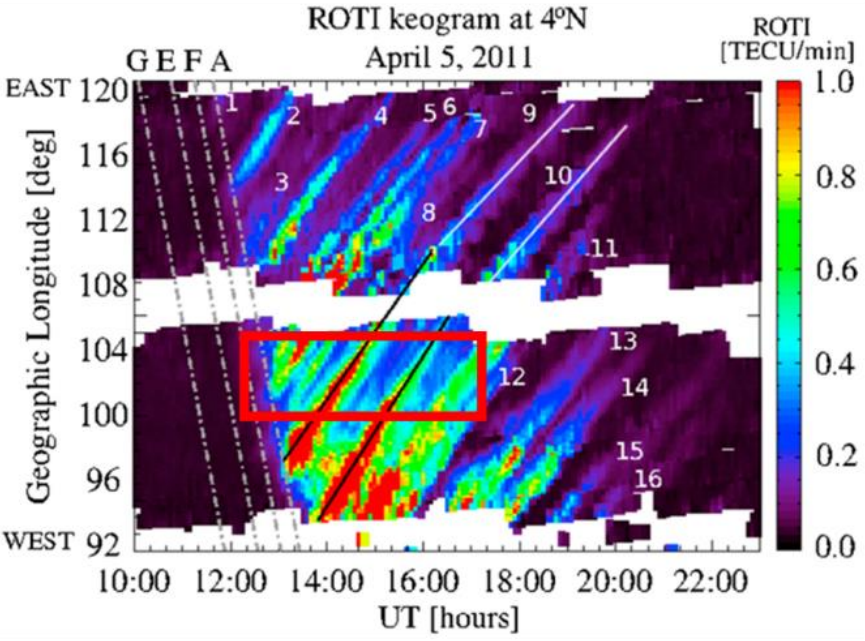


**Figure 3: Detection of EPBs Structure from Buhari Et Al. (2014) Based on ROTI Maps That Covered the Southeast Asian Region Over Latitude 4ºN. The Red Box Highlighted The Focused Area In This Study.**

Based on the figure above, at least three structures of the EPBs, which are EPB-8, EPB9 and EPB-10, has been observed over the study area as highlighted in the red box. It can be categorized the EPB-9 has a large depletion of TEC as its structure shows a thicker formation of EPB and lasted longer compared to EPB-8 and EPB-10. Noted that there is missing plot (white) in the ROTI maps due to no GPS measurements over the area which are located at South China Sea.

Journal of Information System and Technology Management
JISTM
EISSN: 0128-1666
Volume 6 Issue 24 (December 2021) PP. 152-160
DOI: 10.35631/JISTM.624016

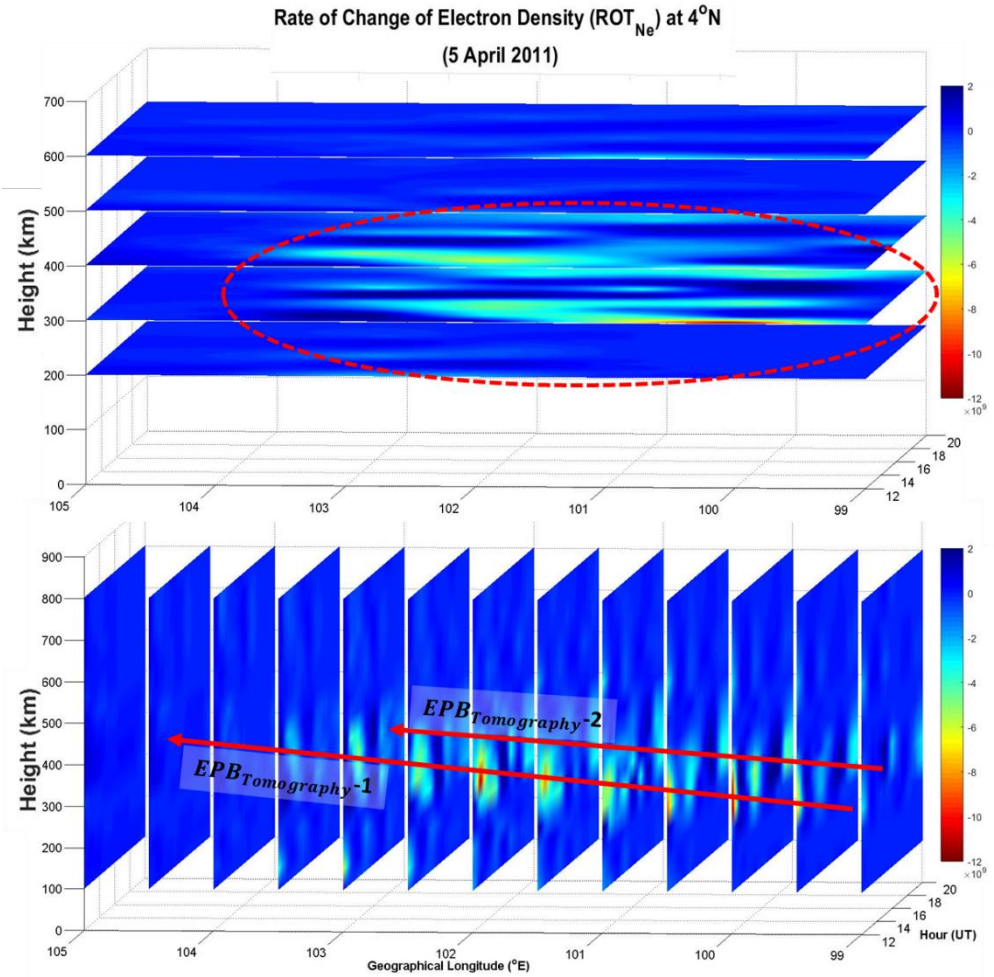


**Figure 4: The ROT$_{Ne}$ Over Cross Section of Latitude 4ºN. The Red Dotted Circle Highlighted the Depletion of Ne Which Represent the EPBs Structure Over the Study Area.**

Figure 4 maps the cross section of the three-dimensional EPBs structure at 4°N using tomography method. It is noted that the structured of the EPBs are highlighted with the red dotted circle and red arrows. Based on the results, it was found that the tomography able to capture at least two EPBs structure out of three EPBs structure over the study area with depletion values up to -12x10$^9$ el/cm. Both structures that were detected grow towards east direction with time and appear stronger across the study area. One of the structures appeared approximately around 12 UT and forming thicker formation of EPB, while another thinning structure later was observed forming around 15 UT.

By comparing the ROT$_{Ne}$ map with ROTI map from Buhari *et al.* (2014), the EPBNe-1 most probably represent the EPB-9 while EPB$_{Ne}$-2 represents EPB-10. This deduction is conclude based on the time occurrences of the EPBs structures as well as its locations. This shows that the tomography is only able to detect the thicker formation of EPBs that occurred over the study area. This shows the capability of the tomography only capable to capture the thicker formation of the EPBs, where the tomography unable to detect the structure of EPB-8.

Journal of Information System and Technology Management
JISTM
EISSN: 0128-1666
Volume 6 Issue 24 (December 2021) PP. 152-160
DOI: 10.35631/JISTM.624016

Based on Huang *et al.* (2012), a weaker structure of the EPBs has a small amount of depletion of electron density and looks thinner. Most likely, this structure has a shorter lifetime and may stop growing at lower altitude. Due to this, it is difficult for tomography to detect the weaker structure of EPBs (i.e., EPB-8). The differences of the numbers of the EPBs structures that were detected by the tomography might be due to the time interval of the reconstruction. The ROTI map from Buhari *et al.* (2014) were estimated for every 5 minutes while the tomography was reconstructed for every 60 minutes.

Overall, the results in this study shows the capability of the GPS ionospheric tomography method to capture the three-dimensional structure of EPBs. This show that the tomography can be utilized in detection and monitoring the ionospheric irregularities especially over the equatorial region.

## Conclusion

This paper presents the reconstruction of the ionospheric tomography in detection of EPBs structure based on the previous case study. The result shows that the tomography capable to detect the structures of the EPBs, especially the stronger structure during the study period. Small fluctuation that occurs unable to be detected due to the large data gap of the reconstruction. Hence, it is recommended to decrease the time gap of the reconstruction to 5 to 30 minutes. Overall, it can be concluded that the GPS ionospheric tomography suitable to be used to capture the signature of EPBs.

## Acknowledgement

The authors would like to express their appreciation to IGS and Department of Survey and Mapping Malaysia (DSMM) for providing the GPS data. This work has been supported by Research Grant University (Q.J130000.2654.15J86).

## References

Aa, E., Zou, S., Eastes, R., Karan, D. K., Zhang, S. R., Erickson, P. J., and Coster, A. J. (2020). Coordinated ground-based and space-based observations of equatorial plasma bubbles. *Journal of Geophysical Research: Space Physics, 125*(1).

Abadi, P., Otsuka, Y. and Tsugawa, T. (2015). Effects of pre-reversal enhancement of ExB drift on the latitudinal extension of plasma bubble in Southeast Asia. *Earth, Planets and Space, 67*(1), 74.

Abdu, M.A. (2016) Electrodynamics of ionospheric weather over low latitudes. *Geoscience Letters, 3* (1), 11.

Amaechi, P. O., Oyeyemi, E. O., Akala, A. O., Falayi, E. O., Kaab, M., Benkhaldoun, Z., and Mazaudier, C. A. (2020). Quiet time ionopheric irregularities over the African equatorial ionization anomaly region. *Radio Science, 55*(8), 1-16.

Buhari, S.M., Abdullah, M., Hasbi, A.M., Otsuka, Y., Yokoyama, T., Nishioka, M. and Tsugawa, T. (2014). Continuous generation and two-dimensional structure of equatorial plasma bubbles observed by high-density GPS receivers in Southeast Asia. *Journal of Geophysical Research: Space Physics,119*(12). 10-569.

Buhari, S.M., Abdullah, M., Yokoyama, T., Hasbi, A.M., Otsuka, Y., Nishioka, M., Bahari, S.A. and Tsugawa, T. (2015). Climatology of Equatorial Plasma Bubble Observed by MyRTKnet over the Years 2008-2013. *Space Science and Communication (IconSpace), 2015 International Conference IEEE.* 101-105.

Journal of Information System and Technology Management
EISSN: 0128-1666
JISTM
Volume 6 Issue 24 (December 2021) PP. 152-160
DOI: 10.35631/JISTM.624016

Fukao, S., Yokoyama, T., Tayama, T., Yamamoto, M., Maruyama, T. and Saito, S. (2006). Eastward traverse of equatorial plasma plumes observed with the Equatorial Atmosphere Radar in Indonesia. *Annales Geophysicae, 24*(5). 1411-1418.

Chin, J. L. (2011). Women and Leadership: Transforming Visions and Current Contexts. *Forum on Public Policy: A Journal of the Oxford Round Table*, (2), 1–12.

Gurram, P., Kakad, B., Bhattacharyya, A., and Pant, T. K. (2018). Evolution of freshly generated equatorial spread F (F-ESF) irregularities on quiet and disturbed days. *Journal of Geophysical Research: Space Physics*, *123*(9), 7710-7725.

Huang, C.S., de La Beaujardiere, O., Roddy, P.A., Hunton, D.E., Ballenthin, J.O. and Hairston., M.R. (2012). Generation and characteristics of equatorial plasma bubbles detected by the C/NOFS satellite near the sunset terminator. *Journal of Geophysical Research: Space Physics, 117*(A11).

Huba, J. D., and Liu, H. L. (2020). Global modelling of equatorial spread F with SAMI3/WACCM-X. *Geophysical Research Letters, 47*(14).

Khamdan, S.S., Musa, T.A. and Buhari, S.M. (2020). Reconstruction of Three-dimensional Ionospheric profiles using tomography technique. In *Proceeding of 8th International Graduate Conference on Engineering, Science and Humanities.*

Khamdan, S.S., Musa, T.A., and Buhari, S.M. (2019). Seasonal Variations of Equatorial Anomaly Crest using GPS Ionospheric Tomography. In *Journal of Physics Conference Series, 1152*(1).

Khamdan, SS. (2018). Mapping Equatorial Ionospheric Profiles Over Peninsular Malaysia using GPS Tomography. *Master Thesis. Universiti Teknologi Malaysia.*

Kil, H. (2015). The Morphology of Equatorial Plasma Bubbles – a review. *Journal of Astronomy and Space Science, 32*(1). 13-19.

Magdaleno, S., Herraiz, M., Altadil, D, and de la Morena, B. (2017). Climatology characterization of equatorial plasma bubbles using GPS data. *Journal of Space Weather and Space Climate, 7*(A3).

Martiningrum, D. R., Yamamoto, M., and Pradipta, R. (2020). Day-to-day Variability of Field-Aligned Irregularities Occurrence in Nighttime F-region Ionosphere over the Equatorial Atmosphere Radar: A Combinatorics Analysis. *Earth and Space Science Open Archive ESSOAr.*

Mersha, M. W., Lewi, E., Jakowski, N., Wilken, V., Berdermann, J., Kriegel, M., & Damtie, B. (2020). A method for automatic detection of plasma depletions by using GNSS measurements. *Radio Science, 55*(3), 1-8.

Nade, D. P., Potdar, S. S., and Pawar, R. P. (2020). Study of Equatorial Plasma Bubbles Using ASI and GPS Systems. In *Geographic Information Systems in Geospatial Intelligence. IntechOpen.*

Nishioka, M., Saito, A. and Tsugawa, T. (2008). Occurrence characteristics of plasma bubble derived from global ground-based GPS receiver networks. J*ournal of Geophysical Research: Space Physics, 113* (A5).

Oryema, B., Jurua, E. and Ssebiyonga, N. (2016). Variations of Crest-to-Trough TEC ratio of the East African Equatorial Anomaly Region. *International Journal of Astrophysics and Space Science. 4*(1). 12-20.

Patel, N. C., Karia, S. P., and Pathak, K. N. (2017). GPS-TEC variation during low to high solar activity period (2010-2014) under the northern crest of Indian equatorial ionization anomaly region. *Positioning, 8*(2), 13.

Journal of Information System and Technology Management
EISSN: 0128-1666
JISTM
**Volume 6 Issue 24 (December 2021) PP. 152-160**
**DOI: 10.35631/JISTM.624016**

Sarudin, I., Hamid, N.S.A., Abdullah, M and Buhari, S.M. (2017). Investigation of zonal velocity of equatorial plasma bubbles (EPBs) by using GPS data. In *Journal of Physics: Conference Series, 852*(1). IOP Publishing.

Timoçin, E., Inyurt, S., Temuçin, H., Ansari, K., & Jamjareegulgarn, P. (2020). Investigation of equatorial plasma bubble irregularities under different geomagnetic conditions during the equinoxes and the occurrence of plasma bubble suppression. *Acta Astronautica, 177*. 341-350.

Tsunoda, R.T. (2010). On equatorial spread F: Establishing a seeding hypothesis. *Journal of Geophysical Research, 115*(A12).

Tsunoda, R.T. (2015). Upwelling: a unit of disturbance in equatorial spread F. *Progress in Earth and Planetary Science, 2*(1). 9.

Yokoyama, T., Fukao, S. and Yamamoto, M. (2004). Relationship of the onset of equatorial F region irregularities with the sunset terminator observed with the Equatorial Atmosphere Radar. *Geophysical Research Letters, 31*(24).

Yokoyama, T., Jin, H., and Shinagawa, H. (2015). West wall structuring of equatorial plasma bubbles simulated by three-dimensional HIRB model. *Journal of Geophysical Research: Space Physics, 120* (10). 8810-8816.